Journal of Cellular Physiology

The P2X7 purinergic receptor in intervertebral disc degeneration

Journal:	*Journal of Cellular Physiology*
Manuscript ID	Draft
Wiley - Manuscript type:	Research Article
Date Submitted by the Author:	n/a
Complete List of Authors:	Penolazzi, Letizia; University of Ferrara, Neuroscience and Rehabilitation Bergamin, Leticia; University of Ferrara, Medical Sciences Lambertini, Elisabetta; University of Ferrara, Neuroscience and Rehabilitation Vultaggio Poma, Valentina; University of Ferrara, Medical Sciences Sarti, Alba Clara; University of Ferrara, Medical Sciences De Bonis, Pasquale; University of Ferrara, Neurosurgery, S. Anna University Hospital, Ferrara Di Virgilio, Francesco; University of Ferrara, Medical Sciences Piva, Roberta; University of Ferrara, Neuroscience and Rehabilitation
Key Words:	intervertebral disc degeneration, inflammation, P2X7 receptor, NLRP3

The P2X7 purinergic receptor in intervertebral disc degeneration

Running Title: The P2X7R in IVDD

Letizia Penolazzi*[1], Leticia Scussel Bergamin*[2], Elisabetta Lambertini[1], Valentina Vultaggio Poma[2], Alba Clara Sarti[2], Pasquale de Bonis[3], Francesco Di Virgilio[2], Roberta Piva[1]

[1] Department of Neuroscience and Rehabilitation, University of Ferrara, 44121 Ferrara, Italy

[2] Department of Medical Sciences, University of Ferrara, 44121 Ferrara, Italy

[3] Neurosurgery Department, Sant'Anna University Hospital, Ferrara, Italy

* These authors contributed equally to this work.

Correspondence

Roberta Piva, PhD, Department of Neuroscience and Rehabilitation, Via Fossato di Mortara, 74, University of Ferrara, 44121 Ferrara, Italy.

Email: piv@unife.it

Abstract

Mechanisms involved in the development of the intervertebral disc (IVD) degeneration are only partially known, thus making implementation of effective therapies very difficult. In this study we investigated P2X7 purinergic receptor (P2X7R), NLRP3 inflammasome and IL-1β expression in IVD specimens at different stages of disease progression, and during the in vitro de-differentiation process of the primary cells derived thereof. We found that P2X7R, NLRP3 and IL-1β expression was higher in the IVD samples at a more advanced stage of degeneration and in the expanded IVD cells in culture which partially recapitulated the in vivo degeneration process. In IVD cells the P2X7R showed a striking nuclear localization, while NLRP3 was mainly cytoplasmic. Stimulation with the semi-selective P2X7R agonist benzoyl ATP together with LPS treatment triggered P2X7R transfer to the cytoplasm and P2X7R/NLRP3 co-localization. Taken together, these findings support pathophysiological evidence that the degenerated disc is a highly inflamed microenvironment, and highlight the P2X7R/NLRP3 axis as a suitable therapeutic target. The immunohistochemical analysis and the assessment of subcellular localization revealed a substantial expression of P2X7R also in normal disc tissue. This gives us the opportunity to contribute to the few studies performed in natively expressed human P2X7R so far, and to understand the possible physiological ATP-mediated P2X7R homeostasis signaling. Therefore, collectively, our findings may offer a new perspective and pave the way for the exploration of a role of P2X7R-mediated purinergic signaling in IVD metabolism that goes beyond its involvement in inflammation.

Keywords: intervertebral disc degeneration, inflammation P2X7 receptor, NLRP3

1 INTRODUCTION

Intervertebral disc degeneration (IVDD), the main cause of lower back pain (LBP) and other spine disorders (Richardson et al., 2014; Vlaeyen et al., 2018), is a multifactorial condition characterized by loss of cellular phenotype, alteration of the extracellular matrix, biomechanical changes and the establishment of an inflamed environment (Dowdell et al., 2017). The entire anatomical structure of the disc is affected by degeneration starting in the nucleus pulposus (NP), a proteoglycan-rich gelatinous tissue located at the center of the intervertebral disc (Shapiro and Risbud, 2014). Degeneration then spreads to the annulus fibrosus (AF), a collagen-rich fibrocartilaginous tissue surrounding the NP, and two cartilaginous endplates that interface with the vertebral bodies (Zhao et sl., 2007). The loss of disc homeostasis is aggravated by a limited self-repair capacity (Ma et al., 2019; Lyu et al., 2019; Shapiro and Risbud, 2014). Today, no efficient therapy is available and current treatments for IVDD are limited to symptom management, such as physical therapies, anti-inflammatory medications, and analgesics. Chronic cases often undergo surgery with controversial outcomes including biomechanical complications and accelerated degeneration of adjacent segments. In recent years important progress has been made in understanding the mechanisms involved in the development of the IVDD, and novel candidate therapies have been proposed (Henry e al., 2018; Clouet et al., 2019). Currently, research focuses on two main aims: 1. develop new therapeutic strategies to mitigate inflammation and the ensuing progressive tissue damage, and 2. stimulate the endogenous repair process. To achieve these aims, therapies targeting newly-discovered catabolic molecules and strategies enhancing the regenerative activity of resident progenitor cells are being implemented. The challenge is the identification of a single molecule or a combination of molecules satisfying both needs. The P2X7 purinergic receptor (P2X7R) might be one such molecules. The underlying reasons prompting this investigation are several: a) the P2X7R, a member of ATP gated ion channel family, has a pleiotropic function in different pathological conditions (Di Virgilio et al., 2018a; Burnstock and Kennedy, 2011; Di Virgilio et al., 2018b; Di Virgilio and Adinolfi, 2017); b) ATP is constantly released from IVD cells exposed to mechanical loading (Wang et al., 2013); c) extracellular (eATP) is a powerful pro-inflammatory agent (Di Virgilio et al., 2019); d) accumulation of adenosine generated by eATP hydrolysis plays a crucial role in maintaining the integrity of the IVD by upregulating the expression of extracellular matrix (ECM) components and by fueling intracellular ATP production in IVD cells in culture (Kerr et al., 2017). In the P2R family,

P2X7R is the subtype mainly involved in the activation and maintenance of inflammation through the activation of the NLRP3 inflammasome and the associated release of cytokines such as interleukin (IL)-1β and IL-18 (Giuliani et al., 2017; Huang et al., 2021; Franceschini et al., 2015; Paik et al., 2021). To date, despite the well-known involvement of IL-1β in the inflammatory response during disc degeneration, NLRP3 and P2X7R have never been correlated in IVDD (Yang et al., 2015; Chao-Yang et al., 2021).

It can be hypothesized that eATP acting at the P2X7R triggers IVDD and support its progression, as described for rheumatoid arthritis, a chronic inflammatory disorder that can affect any joints in the body (Fan et al., 2016; Li et al., 2021). Based on these assumptions, the aim of this study was to investigate the impact of changes in P2X7R, NLRP3 and IL-1β expression during the intervertebral disc degeneration, and during the de-differentiation process of the expanded primary IVD cells in culture. Functionality and subcellular localization of P2X7R was also assessed together with a possible co-localization with the NLRP3 inflammasome.

2 METHODS

2.1 Human Tissue collection and grading

Human lumbar disc tissues were collected from 57 donors (35 males and 22 females, average age, 57.67 years; range, 33–83 years, see Table 1 and supplemental table 1) undergoing spinal surgery for lumbar disc herniation. Degree of IVD degeneration was assessed before spinal surgery using the Pfirrmann MRI-grade system (Pfirrmann et al., 2001). In particular, this grading system consists of five grades of lumbar disc degeneration. Four different parameters were analyzed: Homogeneity of the disc, height of the disc, intensity of disc's signal on the MRI and distinction between the nucleus and anulus. From I grade to V grade of this classification, the lumbar disc appears from homogeneous to inhomogeneous respectively, it decreases its height, from a bright hyperintense white signal intensity it gains a hypointense black signal intensity and the distinction between the nucleus and anulus is progressively lost. Research protocol was approved by Ethics Committee of the University of Ferrara and S. Anna Hospital (protocol approved on 17 November, 2016). All participants provided written informed consent for sample collection before experiments. Every lumbar vertebral disc sample was immediately preserved in sterile saline solution and processed within 24 h from the surgery.

2.2 Isolation of human IVD cells

Lumbar intervertebral disc tissues (1-2 cm^3) were collected, cut into small pieces, and subjected to mild digestion in 15 ml centrifuge tube with only 1 mg/mL type IV collagenase (Sigma Aldrich, St. Louis, USA) for 5 h at 37°C in Dulbecco's Modified Eagle's Medium (DMEM)/F12 (Euroclone S.p.A., Milan, Italy) as previously described (Penolazzi et al., 2018). Once the digestion was terminated, cell suspension was filtered with a Falcon™ 70 µm Nylon Cell strainer (BD Biosciences, Franklin Lakes, NJ, USA). Subsequently 300 xg centrifugation was conducted for 10 min, the supernatant discarded, the cells resuspended in basal medium (DMEM/F12 containing 10% fetal calf serum, 100 µg/mL streptomycin, 100 U/mL penicillin, and 1% Glutamine) (Euroclone) and seeded in polystyrene culture plates (Sarstedt, Nümbrecht, Germany) at a density of 10,000 cells/cm^2. The cells that were released from the dissected tissue and maintained in culture at 37°C in a humidified atmosphere with 5 % CO_2 within the first 48 hours were referred to as passage zero (P0) cells. P0 cells were

expanded by growing for a period not exceeding a week until subconfluent, detaching by trypsinization, and maintained in culture for two passages to obtain P2 cells.

2.3 Histochemical analysis

Small fragments of each IVD sample were rinsed with PBS 1X, fixed in 4% buffered paraformaldehyde for 24 h at 4°C, embedded in paraffin and cross-sectioned (5 µm thick). For histological evaluation sections were immunostained with antibodies against: P2X7R (#APR-004, Alomone Labs, Jerusalem, Israel; 1:50 dilution), NLRP3/NALP3 (#NBP2-12446, Novus Biologicals, Colorado, USA; 1:50 diluition) or IL-1β/IL-1F2 (#NB600-633, Novus Biologicals, 1:100 diluition). Immunohistochemical sections were deparaffnized, rehydrated and heated in sodium citrate (pH 6) for antigen retrieval. Slides were then processed with 3% H_2O_2 in PBS 1X for 5 min and with blocking solution (PBS 1X /1% BSA/10% FCS) for 30 min at room temperature. Then the slides were incubated over night with the primary antibody at 4°C, followed by treatment with Vectastain ABC solution (Vectorlabs) for 30 min. The reactions were developed using DAB solution (Vectorlabs), the sections were counterstained with hematoxylin and mounted in glycerol. The stainings were quantified by a computerized video camera-based image analysis system (NIH, USA ImageJ software, public domain available at: http://rsb.info.nih.gov/nih-image/) under brightfield microscopy (NikonEclipse 50i; Nikon Corporation, Tokyo, Japan). For the analysis of sections, positive cells in the area were counted and protein levels expressed as % of positive nuclei (ten fields per replicate, five sections per sample).

2.4 Quantitative real-time PCR analysis

Total RNA was extracted from IVD cells using the PureLink RNA Mini Kit (ThermoFischer Scientific, Waltham, MA, USA) according to the manufacturer's instructions and RNA content was determined with a Nanodrop 2000 spectrophotometer (ThermoFischer Scientific). RNA was added to each cDNA synthesis reaction using the High Capacity cDNA Reverse Transcription Kit (ThermoFisher Scientific). Real Time PCRs were carried out in the AB StepOne Real Time PCR with TaqMan Gene Expression Master Mix (ThermoFisher Scientific). Amplification was performed with TaqMan Gene Expression Assays for pan-P2X7R (Hs00175721_m1, recognizing both the A and B isoforms of the P2X7R), GAPDH (4326317E) (ThermoFisher Scientific) whereas TaqMan Gene Expression custom assays

(ThermoFisher Scientific) were purchased to identify P2X7RA and P2X7RB previously described by (Adinolfi et al., 2010). Human glyceraldehyde 3-phosphate dehydrogenase (GAPDH) served as the normalizer. The relative gene expression was expressed as fold-change calculated by the $2^{-\Delta\Delta CT}$ method.

2.5 Immunocytochemistry

Immunocytochemistry was performed using the ImmPRESS kit (#MP-7500; Vectorlabs, Burlingame, CA, USA). IVD cells (P0 and P2) were fixed with cold 100% methanol at room temperature (RT) for 10 min and permeabilized with 0.2% (v/v) Triton X-100 in PBS 1X. Cells were treated with 3% H_2O_2 for 10 min (RT), and incubated in blocking solution containing 1% BSA/2.5% FCS for 20 min at RT. After the incubation in blocking solution, the different primary antibodies were added and incubated at 4°C overnight: P2X7R (#APR-004; rabbit anti-human, 1:1000 dilution, Alomone Labs, Jerusalem, Israel), NLRP3/NALP3 (#NBP2-12446, rabbit anti-human, 1:1000 diluition, Novus Biologicals), COL2A1 (#Ab3092; mouse anti-human, 1:200 dilution, Abcam, Cambridge, UK), SOX9 (#sc-20095; rabbit anti-human, Santa Cruz Biotechnology, Texas, USA), ACAN (#sc-33695; mouse anti-human, 1:200 dilution, Santa Cruz Biotechnology), or isotype control (normal rabbit IgG; #2729, 1:1000 dilution, Cell Signaling technology, Massachusetts, USA) were added and the incubation carried out overnight (4°C). Cells were then incubated in Vectastain ABC (Vector Labs) and stained with DAB solution (Vector Labs). After washing, cells were mounted in glycerol/TBS 9:1 and observed with a Leitz microscope (Wetzlar, Germany). Quantitative image analysis of immunostained cells was obtained by a computerized video-camera-based image-analysis system (with NIH USA ImageJ software, public domain available at: http://rsb.info.nih.gov/nih-image) under bright field microscopy. Briefly, images were taken with single stain, without carrying out nuclear counterstaining with hematoxylin and unaltered TIFF images were digitized and converted to black and white picture to evaluate the distribution of relative gray values (i.e., number of pixels in the image as a function of gray value), which reflected chromogen stain intensity. The results were expressed by the quantification of pixels per 100 cells.

2.6 Immunofluorescence

Cells were seeded on glass coverslips put into 24 well plates/ and fixed in 4% paraformaldehyde for 15 min. After three washes with PBS 1X , the cells were permeabilized using 0.05% (v/v) Triton X-100 in PBS 1X for 10 min; then cells were incubated in the blocking solution containing 2% nonfat dry milk -NFDM/0.05% Triton X-100 in PBS 1X for 40 min. After that, cells were incubated overnight at 4° C with the primary antibodies: anti-P2X7R (#P8232, C-ter 576-595 and #P9122, ectodomain 136-152, rabbit anti-human, 1:100 dilution, Sigma Aldrich) and anti-NLRP3 (#AG-20B-0014-C100, mouse anti-human 1:100, Adipogen, San Diego, CA, USA). When required blocking peptide for the P8232 antibody (#AB5246, Merck KGaA, Darmstadt, Germany) was added to the primary antibody at a 1:1 ratio. Then, cells were incubated with the fluorescent secondary antibodies goat anti-rabbit IgG Alexa Fluor 488 (#A11008, 1:1000 dilution, ThermoFisher Scientific) and goat anti-mouse IgG Alexa Fluor 546 (#A11003, 1:1000 dilution, ThermoFisher Scientific) in 2% NFDM/0.05% Triton X-100 in PBS 1X for 1 h at RT. Cells were then washed three times with 0.1% Triton X-100 in PBS. Samples were mounted in ProLong Gold antifade (ThermoFisher Scientific) and images captured with a confocal microscope (LSM 510, Carl Zeiss).

The images were background corrected, and Pearson's coefficient for co-localization was analysed using the JACOP plugin of the open source Fiji software (http://fiji.sc/Fiji).

2.7 Cytosolic free calcium concentration measurements

Cytosolic free calcium was measured using the fluorescent Ca^{2+} indicator Fura-2-acetoxymethyl ester (Fura-2/AM) (ThermoFischer Scientific) (Di Virgilio et al., 2019). IVD cells (P2) were incubated at 37°C for 20 min in saline solution (125 mM NaCl, 5 mM KCl, 1 mM $MgSO_4$, 1 mM NaH_2PO_4, 20 mM HEPES, 5.5 mM glucose, and 5 mM $NaHCO_3$, pH 7.4), in presence of 1 mM $CaCl_2$, and supplemented with 4.0 µM Fura-2/AM and 250 µM sulfinpyrazone (Sigma-Aldrich). Then, the cells were centrifuged at 300 x g for 5 min. The supernatant was discarded and the pellet was resuspended in the above saline solution. The cell suspension was placed in a thermostat-controlled (37°C) and magnetically-stirred cuvette of a Cary Eclipse Fluorescence Spectophotometer (Agilent Technologies, Milan, Italy). The $[Ca^{2+}]_i$ was determined at the 340/380 nm excitation ratio and at 505 nm emission wavelengths. The P2X7R agonist, 2'(3')-*O*-(4-benzoylbenzoyl) ATP (BzATP) (500 µM) (Sigma-Aldrich), was added to investigate P2X7R responses. Ionomycin 1 µM was added to trigger a maximal Ca^{2+} increase.

2.8 Ethidium bromide uptake

Changes in plasma membrane permeability after exposure to BzATP (500 µM) (Sigma-Aldrich) were studied by ethidium bromide uptake. IVD cells were kept at 37°C in a thermostat-controlled and magnetically stirred cuvette of a Cary Eclipse Fluorescence Spectophotometer (Agilent Technologies) in the presence of 20 µM ethidium bromide (Sigma-Aldrich). Fluorescence changes were acquired at 360 nm and 580 nm excitation and emission wavelengths, respectively. Full permeabilization was obtained with 100 µM digitonin.

2.9 Cytokines release

The IVD cells were cultured with DMEM/F-12 medium with 1% FBS for 24 h before treatment and then were treated with 10 ug/ml LPS (Sigma Aldrich) for 24 h. One hour before the end of treatment, the cells were exposed to 500 µM BzATP; After treatment the supernatants were collected and frozen at − 20 °C until further analysis. The evaluation of IL-1β release in cell supernatant was measured by Quantikine Immunoassay for human IL-1β/IL-1F2, purchased from R&D Systems (Minneapolis, USA), as described by the manufacturer. The results were expressed by pg/mL of cytokine/µg/µL of protein.

2.10 Statistical analysis

The data were analyzed for statistical significance by Student's *t*- test or one way ANOVA followed by a post-hoc test for multiple comparisons (Tukey test). Differences were considered significant at $p<0.05$.

3 RESULTS

3.1 P2X7R in intervertebral disc degeneration

Immunohistochemistry of P2X7R was performed on IVD specimens with different Pfirrmann grade of degeneration (see Table 1 for sample information and Supplemental Table 1 for clinical details for each patient) (Pfirrmann et al., 2001). Percentage of P2X7R-positive cells was significantly higher in IVD samples at more advanced stage of degeneration (Figure 1a). On the contrary, a low-level expression of the P2X7R was associated with the lower degeneration stage. This correlation was maintained in primary IVD cells released from the dissected tissue and assayed within 48 h from plating (P0 cells) (Figure 1b). To verify whether P2X7R expression was also affected by the de-differentiation process, gene expression analysis was also performed on expanded IVD cells in culture. As previously reported by us and others (Penolazzi et al., 2018; Rosenzweig et al., 2017), after two passages in culture (P2), IVD cells undergo a de-differentiation process associated with the loss of the chondrocyte-like phenotype, as revealed by decreased expression of typical chondrogenic markers, including collagen type II, SOX9 transcription factor and aggrecan (Supplemental Figure 1). In these de-differentiated cells (P2) P2X7R mRNA expression significantly increased in 5 out 7 samples or remained unchanged (2 out 7) respect to P0 cells (Figure 2a). At least ten splice variants of the human P2X7 subunit are known, of which two, P2X7A (full length isoform) and P2X7B (carboxyl terminal-truncated isoform) are the most common (Adinolfi E et al., 2010; Pegoraro A et al., 2021). By using specific primers we found it is almost exclusively the P2X7A variant that increases during the dedifferentiation process since the P2X7B variant is almost undetectable in IVD cells.

The P2X7R functions both as a cation-selective ion channel and a non-selective pore permeable to high MW aqueous solutes. To assess these responses, IVD cells in culture were challenged with the semi-selective ATP analogue BzATP and cytoplasmic Ca^{2+} changes or ethidium bromide uptake were recorded. P2X7R-dependent responses were negligible since only in one sample out five a BzATP-triggered Ca^{2+} rise was detected, and no cells showed ethidium bromide uptake (Figure 2c).

Considering that the experimental model we are studying is not a system in which P2X7R is artificially expressed, but consists of cells constitutively expressing P2X7R, the techniques used may not be sensitive enough to measure local ionic variations, or the receptor may exert its functions through peculiar mechanisms that would require different methods of investigation.

3.2 Correlation between NLRP3 and IL-1β expression in intervertebral disc degeneration

The involvement of the NLRP3 inflammasome and IL-1β in IVDD has been largely studied, but to date the association between NLRP3 and P2X7R in this disease has not yet been investigated. IVD tissue samples and IVD primary cells therefrom isolated previously used for P2X7R analysis were then investigated for NLRP3 and IL-1β expression. NLRP3 expression was higher in IVD samples with mild (PF III) or high (PF IV-V) Pfirrmann grades of degeneration versus low grades (I-II) (Figure 3a). This correlation was maintained in IVD primary cells at passage P0 (Figure 3b). However, NLRP3 expression did not significantly increase during the de-differentiation process in culture (Figure 3c). Immunostaining revealed that also IL-1β expression increased with the grade of IVD degeneration (Figure 4a). However, IL-1β release evaluated in expanded IVD cells in culture (P2) in culture was more erratic since few IVD cultures (3 out 7) released this cytokine when challenged with the canonical lipopolysaccharide (LPS) plus BzATP stimulation (Figure 4b).

3.3 P2X7R and NLRP3 co-localization

The P2X7R is mainly localized to plasma membrane surface, although anecdotal evidence reports its presence on the nuclear membrane and in the mitochondria (Atkinson et al., 2002; Sarti et al., 2021; Menzies et al., 2013; Martínez-Cuesta et al., 2020). Previous data showed that the P2X7R and NLRP3 co-localize at sub-plasmalemmal sites (Franceschini et al., 2015), thus we set to investigate if these two proteins also interact in IVD cells. As reported in Figure 5, P2X7R staining with two different antibodies raised against different P2X7 subunit epitopes (the carboxyl terminal tail or the ectodomain) showed both a diffuse cytoplasmic and nuclear signal. Both the cytoplasmic and the nuclear signal were abrogated by pre-incubation with a specific blocking peptide, thus validating the specificity of the signal (Supplemental Figure 2). NLRP3 was diffusely distributed in the cytosol but was undetectable in the nucleus. As revealed by Manders' Overlap Coefficient (MOC) as an index of co-localization, the P2X7R and NLRP3 co-localized in the cytoplasm in resting IVD cells, and more so in response to LPS and BzATP.

4 DISCUSSION

Mobility of intervertebral joints is provided by very complex anatomical structures, the intervertebral discs (IVD). Degeneration of this tissue (IVDD), whether due to physiological aging, injury or trauma, is a spine disorder that, to date, remains without cure (Richardson et al., 2014; Vlaeyen et al., 2018). IVDD involves the loss of function of the chondrocyte-like cells of the nucleus pulposus and the progressive onset of an inflamed microenvironment. Understanding its pathogenesis is essential for developing targeted efficient therapies. With this in mind, we focused on the P2X7R, a powerful trigger for NLRP3 inflammasome assembly and IL-1β secretion (Adinolfi et al., 2018; Giuliani et al., 2017), aiming at investigating whether changes in P2X7R, NLRP3 and IL-1β expression occurred during the IVDD and during the de-differentiation process of the expanded primary IVD cells in culture. The degree of disc degeneration was based on the Pfirrmann classification (Pfirrmann et al., 2001). Generally, the population requiring spinal surgery are patients with a high degree of degeneration from grade III to V. Grades I to II are usually classified as healthy discs, with normal disc height and a clear difference between the nucleus and annulus or with minor blurring (Pfirrmann et al., 2001). Based on this grading scale, immunohistochemical analysis revealed that P2X7R, NLRP3 and IL-1β expression was significantly higher in the IVD samples with a more advanced degree of degeneration. This is not surprising as the inflammation characterizes intervertebral disc degeneration, with a boost in cytokine levels, which in turn increases the levels of matrix-degrading enzymes and causes the disc height loss (Shamji et al., 2010; Dowdell et al., 2017). Our data are in keeping with previous reports showing the involvement of the P2X7R in inflammation of the joints (Fan et al., 2016; Li et al., 2021; Zeng et al., 2019). The expression profile for P2X7R and NLRP3 was maintained by IVD primary cells (passage P0) as revealed by immunocytochemical analysis. However, in expanded IVD cells in culture despite the P2X7R gene expression was increased at P2 versus P0, neither NLRP3 expression nor IL-1β secretion was significantly enhanced. This is not surprising as although IVD cells in vitro undergo a de-differentiation process that mimics in vivo degeneration, yet the in vitro microenvironment lacks most of the ingredients of the typical inflammatory microenvironment.

Therefore, as a whole our findings show that the all the components of the P2X7R/NLRP3/IL-1β pathway are present in the IVD, and that they are overexpressed during degeneration. Increasing consensus supports the view that the pathophysiological agent that triggers this pathway, i.e. extracellular ATP, is released to high levels at sites of injury and inflammation (Di Virgilio et al.,

2020), thus is also anticipated to accumulate into the degenerating discs. Currently, there is no direct proof that this nucleotide accumulates in the degenerating spine, but circumstantial evidence from other inflamed tissues, central nervous system included, makes this very likely. On the other hand, ATP is one of the earliest and ubiquitous danger-associated molecular pattern (DAMP) produced in the body at sites of injury, infection or inflammation, thus it would be very unusual if it was not released during IVDD (Kopp et al., 2019; Martínez-Cuesta et al., 2020; Di Virgilio et al., 2019; Qu and Dubyak, 2009). However, the P2X7R participates in multiple inflammation-related responses besides release of cytokines or other inflammatory factors since it is well known that VEGF release (Adinolfi et al., 2012), and therefore angiogenesis, and TGFβ secretion (Monção-Ribeiro et al., 2011), and therefore fibrosis, are also driven by P2X7R stimulation. Thus, we cannot discard the possibility that the P2X7R also participates in the healing attempt in IVDD. After all, the P2X7R is also dubbed a "Dr Jekyll/Mr Hyde" receptor for its ability to mediate both cell injurious and cell trophic events (Di Virgilio, 2000). Should this be the case, controlled activation of the P2X7R by positive allosteric modulators rather than outright inhibition might be an appealing therapeutic option. In particular, the possibility that P2X7R can participate in a controlled pro-fibrotic pathway activating the collagen biosynthetic machinery should not be underestimated. It is in fact important to underline that the presence of progenitor cell populations in the nucleus pulposus has been described, as well as the attempt by these cells to maintain tissue homeostasis and re-establish biomechanical stability (Lyu et al., 2019). This means that an intrinsic repair response to tissue damage is possible, even if an actual healing process fails in most cases. These progenitor cells have also been attributed the ability to produce non-detrimental fibrotic changes as an initial compensatory protective mechanism to preserve the IVD height, through the formation of organized scar tissue necessary for mechanical stability (Lyu et al., 2019; Chen et al., 2020; Frapin et al., 2020; Yang et al., 2021). It is reasonable to assume that P2X7R may support a reparative fibrosis process through two different ways: i. by the inflammasome-mediated secretion of bioactive IL-1β, which stimulates collagen expression and maintains high levels of active TGF-β1 (Ouyang et al., 2013), the master regulator of fibrotic response (Lodyga and Hinz, 2020); or ii. by the activation of the transcriptional machinery. These aspects are consistent both with literature data including the evidence that NLRP3/IL-1β signaling participates in P2X7R-mediated fibrosis in some tissues (Zhou et al., 2020; Gentile et al., 2015), and the presence of P2X7R in the nucleus of IVD cells that we found.

In this scenario considering the possibility of both reverting the degenerated IVD cellular phenotype or sustaining IVD homeostasis by modulating the expression of P2X7R and/or its interacting partners

(Matta et al., 2020; Vergroesen et al., 2015; Zhang et al., 2019), it is crucial to pay attention in the analysis of subcellular localization.

Immunofluorescence and immunocytochemistry showed intense P2X7R specific staining. Two different anti-P2X7 antibodies were used, raised against the carboxyl-terminal or the ectodomain. Both antibodies heavily stained the cell membrane, the cytoplasm and the nucleus. Nuclear localization was unexpected since this receptor is well known to localize at the cell membrane, or to intracellular organelles, such as the endo-lysosomes (Di Virgilio et al., 2017). A previous report shows its localization to the nuclear membrane (Atkinson et al., 2002), thus implying that it might also be present on the endoplasmic reticulum membrane. The P2X7R in the cytoplasm weakly co-localized with NLRP3 in the absence of stimuli, but more strongly when cells were challenged with the canonical NLRP3 stimulants LPS and BzATP. Nearly fifty P2X7R interaction partners have been at least tentatively identified (Kopp et al., 2019; Martínez-Cuesta et al., 2020; Di Virgilio et al., 2019; Qu and Dubyak, 2009), two of them being present in the nucleus, nucleoprotein TPR, a component of the nuclear pore complex, and apoptosis-associated speck-like protein containing a CARD (ASC). Interaction with these proteins might help explain the strong nuclear localization of the P2X7R in IVD cells.

The expression of P2X7R in the nucleus deserves an in depth investigation because it may have far reaching pathophysiological implications both in maintaining disc homeostasis and as a contributing factor to IVDD. Nuclear P2X7R might modulate the transcription of specific genes (Kopp et al., 2019), or act as scaffold protein transmitting mechanical signals across the nuclear envelope (Donnaloja et al., 2019). Recent findings support a direct role of the nucleus in cellular mechanosensing (Kirby and Lammerding, 2018), as well as a possible role of the P2X7R in molecule trafficking across the nuclear envelope (Atkinson et al., 2002; Menzies et al., 2003). Even if mechanotransduction pathways are still incompletely defined in the IVD, it is well known that mechanical loading associated to a change in ATP turnover is a critical regulator of IVD cell activity (Fearing et al., 2018). Therefore, the presence of P2X7R in the nucleus supports its potential role in cellular responses to mechanical stimuli.

IVDD is still an unmet medical need: no efficacious therapy is and even the pathophysiology is poorly known. The P2X7R is gaining increasing attention for its central role in inflammation and immunity. We believe that P2X7R-targeting therapies will be an appealing avenue for IVDD treatment.

FUNDING INFORMATION

This study was supported by Francesco Di Virgilio funds (Italian Association for Cancer Research grants n. IG 13025, IG 18581, IG 22883; the Ministry of Education of Italy grant no. 20178YTNWC), Roberta Piva fund (Fondo per l'Incentivazione della Ricerca – FIR 2020) from University of Ferrara, and Letizia Penolazzi fund (Fondo di Ateneo per la Ricerca Scientifica – FAR 2020) from University of Ferrara.

ACKNOWLEDGEMENTS

We thank Dr. Paola Chiozzi for technical assistance, and Dr. Marta Menegatti for recruitment of IVD samples.

CONFLICT OF INTERESTS

FDV is a Member of the Scientific Advisory Board of Biosceptre Ltd, a UK-based Biotech Company involved in the development of P2X7-targeting antibodies.

Other authors declare no conflict of interests.

AUTHOR CONTRIBUTIONS

Letizia Penolazzi, Leticia Scussel Bergamin, and Elisabetta Lambertini designed the study, performed the experiments and analyzed the data. Valentina Vultaggio Poma and Alba Clara Sarti provided help and advice for the confocal microscopy and acquisition of data. Pasquale de Bonis took care of the clinical aspects and the collection of IVD samples. Roberta Piva and Francesco di Virgilio designed the study, wrote and edited the manuscript. All authors reviewed the manuscript and gave their final approval for submission.

DATA AVAILABILITY STATEMENT

All relevant data are within the article. The data that support the findings of this study are available from the corresponding author upon reasonable request.

REFERENCES

Adinolfi E, Cirillo M, Woltersdorf R, Falzoni S, Chiozzi P, Pellegatti P, Callegari MG, Sandonà D, Markwardt F, Schmalzing G, Di Virgilio F. (2010). Trophic activity of a naturally occurring truncated isoform of the P2X7 receptor. *FASEB J.,* 24(9):3393-3404.

Adinolfi E, Raffaghello L, Giuliani AL, Cavazzini L, Capece M, Chiozzi P, Bianchi G, Kroemer G, Pistoia V, Di Virgilio F. (2012). Expression of P2X7 receptor increases in vivo tumor growth. *Cancer Res.,* 72(12):2957-2969.

Adinolfi E, Giuliani AL, De Marchi E, Pegoraro A, Orioli E, Di Virgilio F. (2018). The P2X7 receptor: A main player in inflammation. *Biochem Pharmacol*., 151:234-244.

Atkinson L, Milligan CJ, Buckley NJ, Deuchars J. (2002). An ATP-gated ion channel at the cell nucleus. *Nature*, 420(6911):42.

Bergamin LS, Penolazzi L, Lambertini E, Falzoni S, Sarti AC, Molle CM, Gendron FP, De Bonis P, Di Virgilio F, Piva R. (2021). Expression and function of the P2X7 receptor in human osteoblasts: The role of NFATc1 transcription factor. *J Cell Physiol.,* 236(1):641-652.

Burnstock G, Kennedy C. (2011). P2X receptors in health and disease. *Adv Pharmacol.,* 61:333-372.

Chao-Yang G, Peng C, Hai-Hong Z. (2021). Roles of NLRP3 inflammasome in intervertebral disc degeneration. *Osteoarthritis Cartilage*., 29(6):793-801.

Chen C, Zhou T, Sun X, Han C, Zhang K, Zhao C, Li X, Tian H, Yang X, Zhou Y, Chen Z, Qin A, Zhao J. (2020). Autologous fibroblasts induce fibrosis of the nucleus pulposus to maintain the stability of degenerative intervertebral discs. *Bone Res.,* 8(1):7.

Clouet J, Fusellier M, Camus A, Le Visage C, Guicheux J. (2019). Intervertebral disc regeneration: From cell therapy to the development of novel bioinspired endogenous repair strategies. *Adv Drug*

Deliv Rev., 146:306-324.

Di Virgilio F. (2000). Dr. Jekyll/Mr. Hyde: the dual role of extracellular ATP. *J Auton Nerv Syst.,* 81(1-3):59-63.

Di Virgilio F, Adinolfi E. (2017). Extracellular purines, purinergic receptors and tumor growth. *Oncogene,* 36(3):293-303.

Di Virgilio F, Dal Ben D, Sarti AC, Giuliani AL, Falzoni S. (2017). The P2X7 Receptor in Infection and Inflammation. *Immunity.* 2017 Jul 18;47(1):15-31.

Di Virgilio F, Giuliani AL, Vultaggio-Poma V, Falzoni S, Sarti AC. (2018). Non-nucleotide Agonists Triggering P2X7 Receptor Activation and Pore Formation. *Front Pharmacol.,* 9:39. (a)

Di Virgilio F, Schmalzing G, Markwardt F. (2018). The Elusive P2X7 Macropore. *Trends Cell Biol.,* 28(5):392-404. (b)

Di Virgilio F, Jiang LH, Roger S, Falzoni S, Sarti AC, Vultaggio-Poma V, Chiozzi P, Adinolfi E. (2019). Structure, function and techniques of investigation of the P2X7 receptor (P2X7R) in mammalian cells. *Methods Enzymol.,* 629:115-150.

Di Virgilio F, Sarti AC, Coutinho-Silva R. (2020). Purinergic signaling, DAMPs, and inflammation. *Am J Physiol Cell Physiol*., 318(5):C832-C835.

Donnaloja F, Jacchetti E, Soncini M, Raimondi MT. (2019). Mechanosensing at the nuclear envelope by nuclear pore complex stretch activation and its effect in physiology and pathology. *Front Physiol.*, 10:896.

Dowdell J, Erwin M, Choma T, Vaccaro A, Iatridis J, Cho SK. (2017). Intervertebral disk degeneration and repair. *Neurosurgery*, 80:S46–S54.

Fan ZD, Zhang YY, Guo YH, Huang N, Ma HH, Huang H, Yu HG. (2016). Involvement of P2X7 receptor signaling on regulating the differentiation of Th17 cells and type II collagen-induced arthritis in mice. *Sci Rep*. 6:35804.

Fearing BV, Hernandez PA, Setton LA, Chahine NO. (2018). Mechanotransduction and cell biomechanics of the intervertebral disc. *JOR Spine.* 1(3):e1026.

Franceschini A, Capece M, Chiozzi P, Falzoni S, Sanz JM, Sarti AC, Bonora M, Pinton P, Di Virgilio F. (2015). The P2X7 receptor directly interacts with the NLRP3 inflammasome scaffold protein. *FASEB J*., 29(6):2450-2461.

Frapin L, Clouet J, Chédeville C, Moraru C, Samarut E, Henry N, André M, Bord E, Halgand B, Lesoeur J, Fusellier M, Guicheux J, Le Visage C. (2020). Controlled release of biological factors for endogenous progenitor cell migration and intervertebral disc extracellular matrix remodelling. *Biomaterials*. 253:120107.

Gentile D, Natale M, Lazzerini PE, Capecchi PL, Laghi-Pasini F. (2015). The role of P2X7 receptors in tissue fibrosis: a brief review. *Purinergic Signal*.,11(4):435-440.

Giuliani AL, Sarti AC, Falzoni S, Di Virgilio F. (2017). The P2X7 Receptor-Interleukin-1 Liaison. *Front Pharmacol.,* 16;8:123.

Huang Z, Xie N, Illes P, Di Virgilio F, Ulrich H, Semyanov A, Verkhratsky A, Sperlagh B, Yu SG, Huang C, Tang Y. (2021). From purines to purinergic signalling: molecular functions and human diseases. *Signal Transduct Target Ther*., 6(1):162.

Kerr GJ, Veras MA, Kim MK, Séguin CA. (2017). Decoding the intervertebral disc: Unravelling the complexities of cell phenotypes and pathways associated with degeneration and mechanotransduction. *Semin Cell Dev Biol.,* 62:94-103.

Kirby TJ, Lammerding J. (2018). Emerging views of the nucleus as a cellular mechanosensor. *Nat Cell Biol.*, 20(4):373-381.

Kopp R, Krautloher A, Ramírez-Fernández A, Nicke A. (2019). P2X7 interactions and signaling - making head or tail of it. *Front Mol Neurosci*.,12:183.

Li Z, Huang Z, Bai L. (2021). The P2X7 Receptor in Osteoarthritis. *Front Cell Dev Biol*., 9:628330.

Lodyga M, Hinz B. (2020). TGF-beta1 - A truly transforming growth factor in fibrosis and immunity. *Semin Cell Dev Biol*. 101:123-139.

Lyu FJ, Cheung KM, Zheng Z, Wang H, Sakai D, Leung VY. (2019) IVD progenitor cells: A new horizon for understanding disc homeostasis and repair. *Nat Rev Rheumatol.*, 15:102-112.

Ma K, Chen S, Li Z, Deng X, Huang D, Xiong L, Shao Z. (2019). Mechanisms of endogenous repair failure during intervertebral disc degeneration. *Osteoarthritis Cartilage*., 27(1):41-48.

Menzies J, Paul A, Kennedy C. (2003). P2X7 subunit-like immunoreactivity in the nucleus of visceral smooth muscle cells of the guinea pig. *Auton Neurosci*., 106(2):103-109.

Martínez-Cuesta MÁ, Blanch-Ruiz MA, Ortega-Luna R, Sánchez-López A, Álvarez Á. (2020). Structural and functional basis for understanding the biological significance of P2X7 receptor. *Int J Mol Sci.,* 21(22):8454.

Matta A, Erwin WM. (2020). Injectable biologics for the treatment of degenerative disc disease. *Curr Rev Musculoskelet Med*., 13(6):680-687.

Monção-Ribeiro LC, Cagido VR, Lima-Murad G, Santana PT, Riva DR, Borojevic R, Zin WA, Cavalcante MC, Riça I, Brando-Lima AC, Takiya CM, Faffe DS, Coutinho-Silva R. (2011). Lipopolysaccharide-induced lung injury: role of P2X7 receptor. *Respir Physiol Neurobiol*., 179(2-3):314-325.

Ouyang X, Ghani A, Mehal WZ. (2013). Inflammasome biology in fibrogenesis. *Biochim Biophys Acta*., 1832(7):979-988.

Paik S, Kim JK, Silwal P, Sasakawa C, Jo EK. (2021). An update on the regulatory mechanisms of NLRP3 inflammasome activation. *Cell Mol Immunol*., 18(5):1141-1160.

Pegoraro A, De Marchi E, Adinolfi E. (2021). P2X7 Variants in Oncogenesis. *Cells* 10 (1): 189.

Penolazzi L, Lambertini E, Bergamin LS, Roncada T, De Bonis P, Cavallo M, Piva R. (2018). MicroRNA-221 silencing attenuates the degenerated phenotype of intervertebral disc cells. *Aging.*, 10:2001-2015.

Pfirrmann CW, Metzdorf A, Zanetti M, Hodler J, Boos N. (2001). Magnetic resonance classification of lumbar intervertebral disc degeneration. *Spine*., 26:1873-1878.

Qu Y, Dubyak GR. (2009). P2X7 receptors regulate multiple types of membrane trafficking responses and non-classical secretion pathways. *Purinergic Signal.,* 5(2):163-173.

Richardson SM, Freemont AJ, Hoyland JA. (2014). Pathogenesis of intervertebral disc degeneration. In: Shapiro I.M., Risbud M.V., editors. *The Intervertebral Disc-Molecular and Structural Studies of the Disc in Health and Disease*. Springer; Vienna, Austria, 177-200.

Rosenzweig DH, Tremblay Gravel J, Bisson D, Ouellet JA, Weber MH, Haglund L. (2017). Comparative analysis in continuous expansion of bovine and human primary nucleus pulposus cells for tissue repair applications. *Eur Cell Mater.*, 33:240-251.

Sarti AC, Vultaggio-Poma V, Falzoni S, Missiroli S, Giuliani A, Boldrini P, Bonora M, Faita F, Di Lascio N, Kusmic C, Solini A, Novello S, Morari M, Rossato M, Wieckowski MR, Giorgi C, Pinton P, Di Virgilio F. (2021) Mitochondrial P2X7 Receptor Localization Modulates Energy Metabolism Enhancing Physical Performance. Function, 2 (2):zqab005.

Shamji MF, Setton LA, Jarvis W, So S, Chen J, Jing L, Bullock R, Isaacs RE, Brown C, Richardson WJ. (2010). Proinflammatory cytokine expression profile in degenerated and herniated human intervertebral disc tissues. *Arthr Rheum.* 62:1974-1982.

Shapiro IM, Risbud MV (2014). Introduction to the structure, function, and comparative anatomy of the vertebrae and the intervertebral disc. In: Shapiro I.M., Risbud M.V., editors. *The Intervertebral Disc-Molecular and Structural Studies of the Disc in Health and Disease*. Springer; Vienna, Austria, pp. 3–16.

Vergroesen PP, Kingma I, Emanuel KS, Hoogendoorn RJ, Welting TJ, van Royen BJ, van Dieën JH, Smit TH. (2015). Mechanics and biology in intervertebral disc degeneration: A vicious circle. *Osteoarthr Cartil*., 23:1057-1070.

Vlaeyen JWS, Maher CG, Wiech K, Van Zundert J, Meloto CB, Diatchenko L, Battié MC, Goossens M, Koes B, Linton SJ. (2018). Low back pain. *Nat Rev Dis Primers*., 2018, 4(1):52.

Wang C, Gonzales S, Levene H, Gu W, Huang CY. (2013). Energy metabolism of intervertebral disc under mechanical loading. *J Orthop Res.,* 31(11):1733-1738.

Yang W, Yu XH, Wang C, He WS, Zhang SJ, Yan YG, Zhang J, Xiang YX, Wang WJ. (2015). Interleukin 1β in intervertebral disk degeneration. *Clin Chim Acta*., 450:262-272.

Yang X, Chen Z, Chen C, Han C, Zhou Y, Li X, Tian H, Cheng X, Zhang K, Qin A, Zhou T, Zhao J. (2021). Bleomycin induces fibrotic transformation of bone marrow stromal cells to treat height loss of intervertebral disc through the TGFβR1/Smad2/3 pathway. *Stem Cell Res Ther.*, 12(1):34.

Zeng D, Yao P, Zhao H. (2019). P2X7, a critical regulator and potential target for bone and joint diseases. *J Cell Physiol*., 234(3):2095-2103.

Zhang Y, Zhang YS, Li XJ, Huang CR, Yu HJ, Yang XX, Wang BX. (2019) Overexpression of miR-150 Inhibits the NF-κB Signal Pathway in Intervertebral Disc Degeneration through Targeting P2X7.Cells *Tissues Organs.* 207(3-4):165-176.

Zhao CQ, Wang LM, Jiang LS, Dai LY. (2007) The cell biology of intervertebral disc aging and degeneration. *Ageing Res Rev.,* 6, 247-261.

Zhou J, Tian G, Quan Y, Li J, Wang X, Wu W, Li M, Liu X. (2020). Inhibition of P2X7 purinergic receptor ameliorates cardiac fibrosis by suppressing NLRP3/IL-1β pathway. *Oxid Med Cell Longev*., 2020:7956274.

FIGURE LEGENDS

Figure 1. P2X7R expression in intervertebral disc. (a), immunohistochemical analysis of P2X7R performed on IVD tissues at different Pfirrmann grade. Quantification was reported and expressed as % of positive cells per area (3-5 sections per sample; Pfirrmann I-II group, n = 7; Pfirrmann III group, n = 8; Pfirrmann IV-V group, n = 12). * $p < 0.01$ (Pfirrmann IV-V group vs Pfirrmann I-II group and Pfirrmann III group vs Pfirrmann I-II). Scale bars: 20 µm. (b), immunocytochemical analysis of P2X7R evaluated on IVD cells (p0) isolated from IVD tissues with different Pfirrmann grade. Protein levels were quantified by densitometric analysis and expressed as means of pixels per one hundred cells ± SD (n = 10). * $p < 0.05$ (Pfirrmann IV-V group vs Pfirrmann I-II group and Pfirrmann III group vs Pfirrmann I-II); ** $p < 0.05$ (Pfirrmann IV-V group vs Pfirrmann III group). Scale bars: 20 µm.

Figure 2. P2X7R expression and function in IVD cells. During de-differentiation process from passage 0 (P0) to passage 2 (P2) P2X7R expression was analyzed. (a), the cells were subjected to RT-PCR, the expression was normalized against GAPDH as endogenous control, and calculated as fold change vs P0 (mean± SD). Data were analyzed by Student's t- test, * $p <0.05$, significantly different from P0 (P0 group, n = 10; P2 group, n = 10). The cells were subjected to RT-PCR (b) for investigating the presence of P2X7RA and P2X7RB isoforms. For mRNA analysis, data were normalized against GAPDH as endogenous control, calculated as change vs P2X7RA (P0) and expressed as mean± SD. Data were analyzed by Student's t- test, *$p <0.05$ significantly different from P0 (P0 group, n = 7; P2 group, n = 7). (c), IVD cells were subjected to P2X7R function analysis. Representative traces showing the increment of intracellular calcium (on the left) and ethidium bromide uptake (on the right), following 500 µM BzATP stimulation (n=5).

Figure 3. NLRP3 expression in intervertebral disc and IVD cells. (a), immunohistochemical analysis of NLRP3 performed on IVD tissues at different Pfirrmann grade. Quantification was also reported and expressed as % of positive cells per area (3-5 sections per sample; Pfirrmann I-II group, n = 7; Pfirrmann III group, n = 8; Pfirrmann IV-V group, n = 12). * $p < 0.01$ (Pfirrmann IV-V group vs Pfirrmann I-II group and Pfirrmann III group vs Pfirrmann I-II). Scale bars: 20 µm. (b), immunocytochemical analysis of NLRP3 evaluated on IVD cells (p0) isolated from IVD tissues with different Pfirrmann grade. Protein levels were quantified by densitometric analysis and expressed as means of pixels per one hundred cells ± SEM (n = 10). * $p < 0.05$ (Pfirrmann IV-V group vs

Pfirrmann I-II group and Pfirrmann III group vs Pfirrmann I-II); ** $p < 0.05$ (Pfirrmann IV-V group vs Pfirrmann III group). Scale bars: 20 µm. (c), NRLP3 expression was analyzed in IVD cells during de-differentiation process from passage 0 (P0) to passage 2 (P2) by immunocytochemistry, quantified by densitometric analysis and expressed as fold change vs P0 (mean± SEM).

Figure 4. IL1-β in intervertebral disc. (a), immunohistochemical analysis of IL1-β performed on IVD tissues at different Pfirrmann grade. Quantification was also reported and expressed as % of positive cells per area (3-5 sections per sample; Pfirrmann I-II group, n = 7; Pfirrmann III group, n = 7; Pfirrmann IV-V group, n = 8). * $p < 0.01$ (Pfirrmann IV-V group vs Pfirrmann I-II group and Pfirrmann III group vs Pfirrmann I-II). Scale bars: 20 µm. (b), IL-1β release by IVD cells after treatment with 500 µM BzATP in the presence of 10 µg/mL LPS. Data are presented as average mean ±SEM. Data were evaluated by ANOVA followed by Tukey test, $p < 0.05$, (n=5).

Figure 5. P2X7R and NLRP3 colocalization in IVD cells. Average Manders colocalization coefficients (± SEM) was evaluated in control cells (CTR) or after treatment with 10 µg/mL LPS+ 500 µM BzATP. * $p < 0.0001$. Representative images were also reported. P2X7R (Alexafluor 488, green); NLRP3 (Alexafluor 546, red). Scale bars: 10 µm.

Table 1. Human IVD samples information.

Age	
Mean (± SD)	57,67 (± 13,44)
Min-Max	33-83

Gender	**n**	**%**
Male	35	61,40
Female	22	38,60

Disc degeneration grade (Pfirrmann)	**n**	**%**
PF I-II	11	19,30
PF III	22	38,60
PF IV-V	24	42,11

Duration symptoms prior to surgery	**n**	**%**
0-3 months	29	50,88
3-6 months	13	22,81
6-12 months	9	15,79
12+ months	6	10,52

Experimental Analysis	**n**	**%**
IHC	27	47,37
IC/IF	25	43,86
Functionality	18	31,57
qPCR	12	21,05

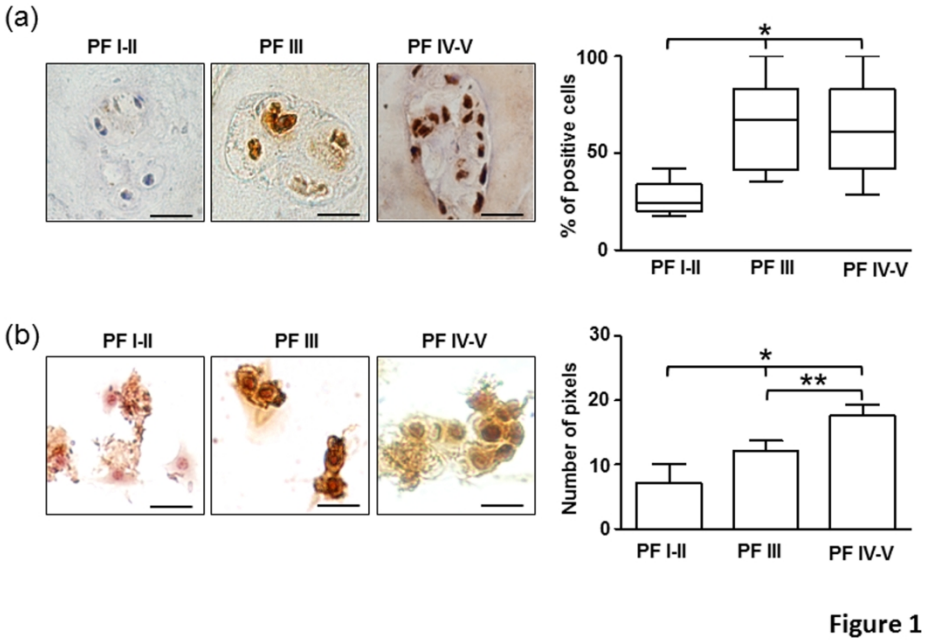

Figure 1

Figure 1

180x126mm (300 x 300 DPI)

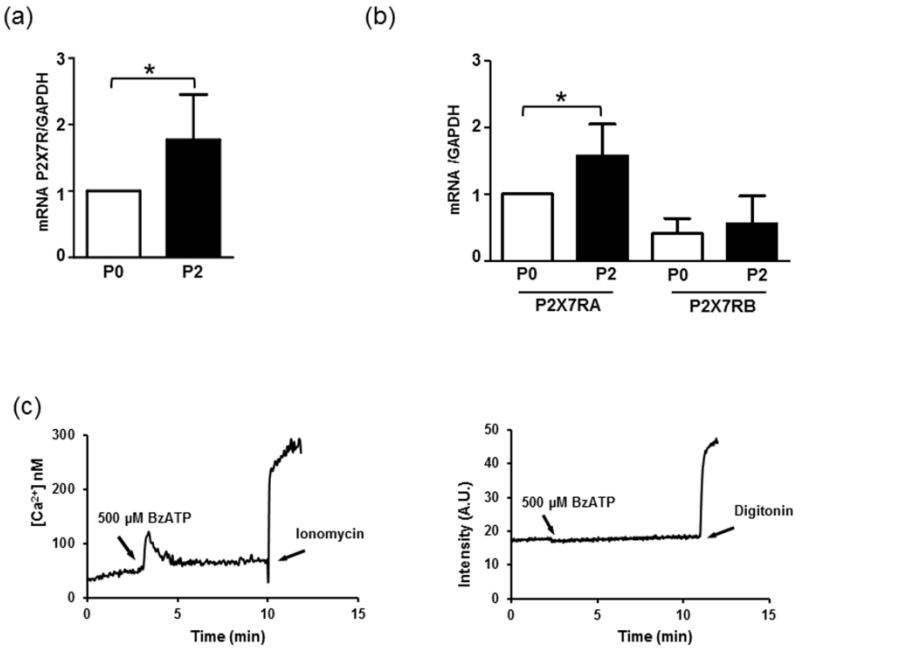

Figure 2

Figure 2

180x134mm (300 x 300 DPI)

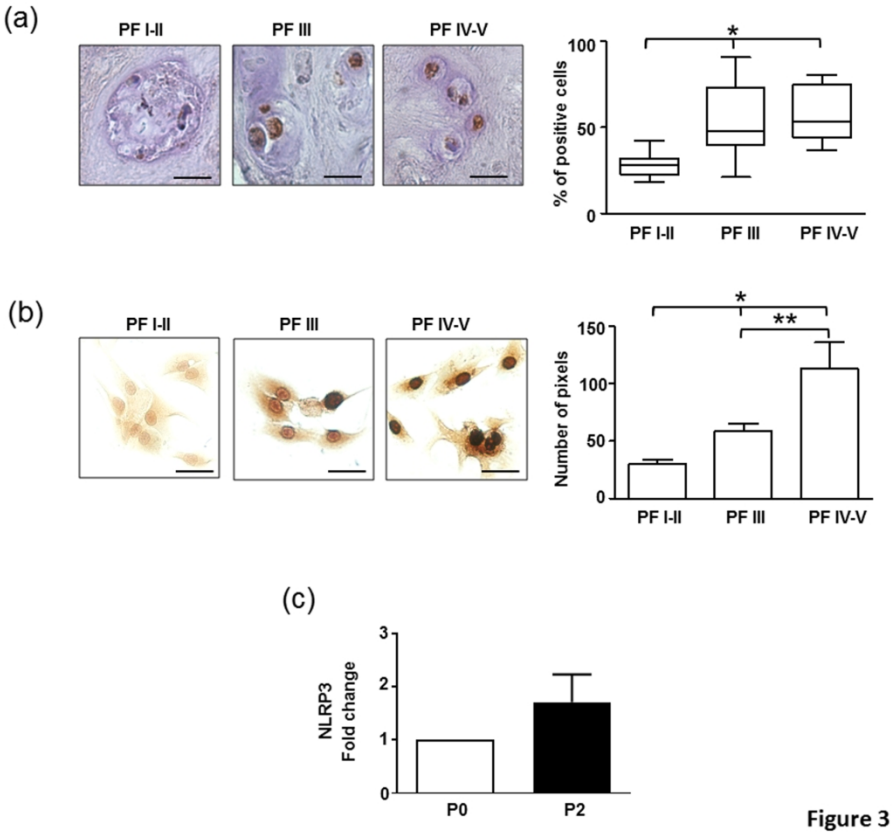

Figure 3

Figure 3

180x165mm (300 x 300 DPI)

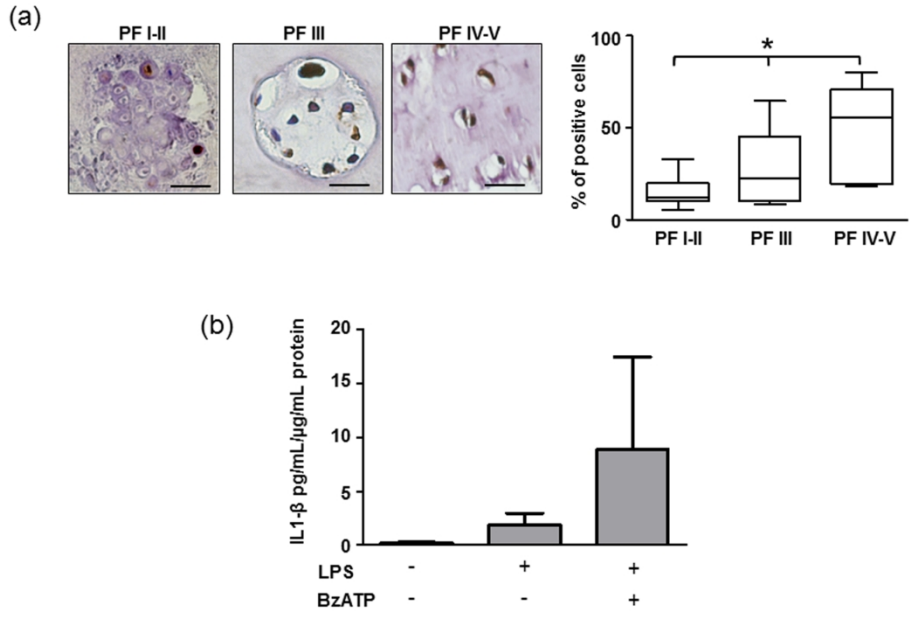

Figure 4

Figure 4

180x137mm (300 x 300 DPI)

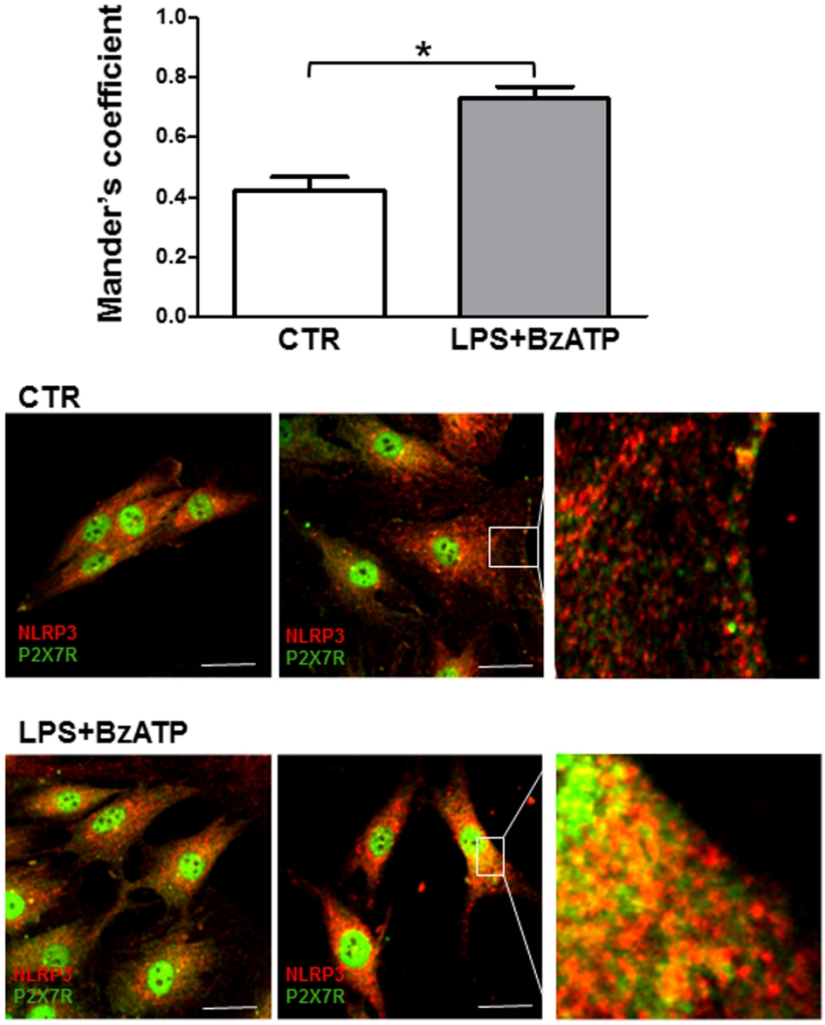

Figure 5

Figure 5

180x208mm (300 x 300 DPI)